Frame Repetition: A Solution to Imaginary Interference Cancellation in FBMC/OQAM Systems

Dejin Kong, Xing Zheng, and Tao Jiang, *Fellow, IEEE*

***Abstract*—In this paper, we propose a complex-valued symbol based FBMC/OQAM (C-FBMC/OQAM) system to achieve the self-cancellation of intrinsic imaginary interference. The key idea is the employment of a well-designed repeated frame, in which complex-valued QAM symbols are transmitted instead of only real-valued symbols in the classical FBMC/OQAM systems. It is proven that, intrinsic interference among symbols can be completely eliminated in the proposed C-FBMC/OQAM systems, and the spectral efficiency is maintained even in the existence of repeated frame. Simulation results shows that the proposed C-FBMC/OQAM system and preamble structures for channel estimation demonstrate improved robustness against frequency selective fading channels compared to conventional FBMC/OQAM systems due to the intrinsic interference cancellation.**

***Index Terms*—FBMC/OQAM, imaginary interference, data reconstruction, complex-valued symbols, frame repetition, frequency selective fading channel.**

I. Introduction

As a viable alternative to orthogonal frequency division multiplexing (OFDM), filter bank multi-carrier with offset quadrature amplitude modulation (FBMC/OQAM) [?], [?], [?] has illustrated compelling advantages over conventional modulation schemes owing to the adoption of prototype filters [?]. Firstly, higher transmission rate and spectral efficiency could be achieved in the absence of cyclic prefix (CP) [?], [?]. Besides, the good time-frequency localization (TFL) properties of prototype filters offers an effective suppression to spectrum sidelobes [?], [?], allowing for the cognitive radio (CR) networks [?], [?], coexisting communication scenes [?], [?] and opportunistic transmissions on fragmented spectrum [?]. Furthermore, the TFL nature also presents an increased resilience against time and frequency misalignment compared to OFDM systems, making it feasible for the appliance to asynchronous scenarios [?]. The outstanding properties mentioned above facilitate FBMC/OQAM being the focus of multiple communication projects [?], [?], [?].

However, all the merits presented above are derived at the cost of sacrificing orthogonality. The orthogonal condition only holds in real field [?], and the QAM symbols are partitioned into real and imaginary parts and transmitted as a pair of real-valued pulse amplitude modulated (PAM) symbols in FBMC/OQAM systems. The relaxation of orthogonality results in intrinsic imaginary interference among symbols [?], [?], which complicates signal processing tasks at the receiver, including channel estimation, equalization and synchronization [?], [?]. Even worse, the existence of imaginary interference leads to the maladjustment of FBMC in maximum likelihood (ML) detection [?], singular value decomposition (SVD) precoding [?], Alamouti space time block coding (STBC) [?], which makes FBMC unsuitable in multiple-input multiple-output (MIMO) applications.

In literature, much work has been done for intrinsic interference cancellation, which can be grouped into two categories, i.e., interference approximation method (IAM) [?], [?], [?], [?], [?], [?], [?], [?], [?] for pilot symbols and filter bank multi-carrier with quadrature amplitude modulation (FBMC/QAM) [?], [?], [?], [?] for data symbols. The IAM was proposed to eliminate the interference to pilot symbols for channel estimation, by placing zeros or known symbols around pilot symbols. Therefore, the preamble in the IAM consists of three column of real-valued symbols, resulting in a larger pilot overhead compared to OFDM systems. Several variants of IAM were proposed to improve the performance of the channel estimation by optimizing the power of pseudo pilot [?], [?], [?], [?]. Furthermore, scattered based pilot structures, i.e. AP [?], CAP [?] were proposed to reduce pilot overheads, in which the frequency flat-fading assumption is still required. Different from IAM, FBMC/QAM aims to mitigate intrinsic interference among data symbols to enable the transmission of complex-valued QAM symbols for simplifying the signal processing at the receiver. The FBMC/QAM structure was firstly proposed in [?] by adopting a truncated filter on the subcarriers with pilots, in which a soft demapper was employed to cope with residual intrinsic interference. In [?], the prototype filters on the even and odd-numbered subcarriers are designed by sacrificing the power spectrum density (PSD) performance to achieve a sub-block wise reverse ordering for intrinsic interference neutralization, making it easier for adjustment to MIMO scenarios. In [?], a decision feedback equalization(DFE)-based FBMC/QAM system was put forward for intrinsic interference mitigation by performing spectral factorization to the system response. In [?], a linearly processed filter-bank multi-carrier (LP-FBMC) was presented, which employed SVD to convert the overlapped FBMC data into parallel independent data for intrinsic interference cancellation. However, compared with FBMC/OQAM systems, the DFE-based FBMC/QAM and LP-FBMC systems suffered from the problems of extra complexity and loss in bit error rate (BER) performance.

In this paper, we propose a novel complex-valued symbols

Dejin Kong, Xing Zheng, Tao Jiang (corresponding author) are with the School of Electronic Information and Communications, Huazhong University of Science and Technology, Wuhan, 430074, China(e-mail: kdjin@hust.edu.cn; xingzheng@hust.edu.cn; tao.jiang@ieee.org)

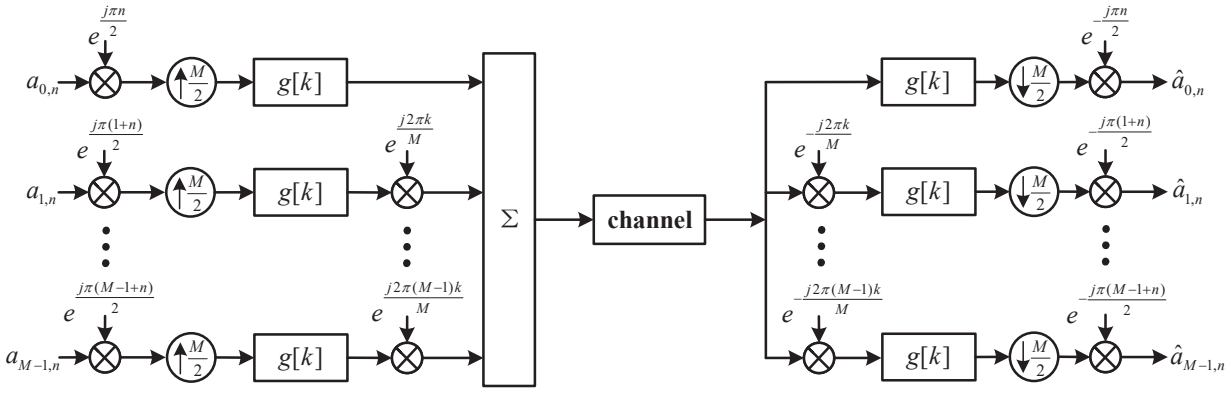

Fig. 1. The equivalent baseband block diagram of an FBMC/OQAM system.

based FBMC/OQAM system (C-FBMC/OQAM) for intrinsic interference cancellation by adopting a well-designed repeated frame structure, in which the spectral efficiency and out-of-band (OOB) emission performance are maintained compared to FBMC/OQAM systems. Besides, we present two channel estimators based on imaginary interference cancellation on pilots in FBMC/OQAM system, which improves the robustness against frequency flat-fading channels compared to the conventional IAM. Mean square error (MSE) and BER, as the performance metric, are used in this paper to evaluate the accuracy channel estimation and data reconstruction of the proposed C-FBMC/OQAM systems and channel estimators, respectively.

To show the novelty of this proposed C-FBMC/OQAM, the main differences between C-FBMC/OQAM and the FBMC/QAM systems are summarized,

- The proposed C-FBMC/OQAM satisfies the orthogonality condition strictly. However, the orthogonality condition of FBMC/QAM is relaxed due to the changes of prototype filters, therefore the intrinsic interference cannot be completely mitigated in FBMC/QAM system even under distortion-free channels.
- The proposed C-FBMC/OQAM exhibits the same PSD and spectral efficiency compared with the classic FBMC/OQAM. However, FBMC/QAM suffers from loss in terms of PSD and spectral efficiency due to the redesign of filters.
- The proposed C-FBMC/OQAM employs the same symbol interval as that in FBMC/OQAM, in which QAM symbols are partitioned into two identical parts and transmitted in the original and repeated frames, respectively. However, the symbol interval in FBMC/QAM is the as that in OFDM, which is twice as that in the proposed C-FBMC/OQAM.

The remainder of this paper is organized as follows. In section II, FBMC/OQAM systems and channel estimation theory in frequency domain are briefly introduced. In section III, the symmetry property of imaginary interference is analyzed and the self-interference cancellation based channel estimators for FBMC/OQAM systems with the structure of repeated frames are proposed. In section IV, the proposed C-FBMC/OQAM system following with its performance analysis is detailed. Simulation results are presented in section V and the work are concluded in section VI.

$Notations$: Upper (lower) bold face letters denote matrices (column vectors). The superscript $(\cdot)^T$ and $(\cdot)^H$ stand for transpose and Hermitian operator, respectively. $\Re(\cdot)$ and $(\cdot)^*$ are respectively the real part and conjugate of a complex number or matrix. $\sqrt{-1}$ is denoted by j. $h[k] * s[k]$ denotes the convolution operation of $h[k]$ and $s[k]$. The symbol δ_{m,m_0} is 1 if $m = m_0$ and 0 otherwise.

II. System Model

A. FBMC/OQAM System Model

Fig. 1 presents the equivalent baseband block diagram of an FBMC/OQAM system with M subcarriers and subcarrier spacing $1/T$, where T is the complex symbol interval in time domain. The real and imaginary parts of each QAM symbols are partitioned, and transmitted as a pair of real-valued PAM symbols with the interval $T/2$. The PAM symbol at frequency index m and time index n is denoted as $a_{m,n}$, therefore $a_{m,2k}$ and $a_{m,2k+1}$, with integer k, are the real and imaginary parts originated from the same QAM symbol, respectively. Generally, the prototype filter is assumed to be symmetrical and real-valued in FBMC/OQAM system (**?**) , which is denoted as $g[k]$ in this paper. The length of the prototype filter is KM, where K is the overlapping factor, usually taking a value of 4 [**?**]. The equivalent baseband FBMC/OQAM signal is given as [**?**], [**?**]

$$s[k] = \sum_{m=1}^{M} \sum_{n\in\mathbb{Z}} a_{m,n} \underbrace{g\left[k - n\frac{M}{2}\right] e^{j2\pi mk/M} e^{j\pi(m+n)/2}}_{g_{m,n}[k]}. \tag{1}$$

For a distortion-free channel, the received signal $r[k] = s[k]$. At the receiver side, the demodulated symbol at the position (m, n) are obtained as

$$\hat{a}_{m,n} = \sum_{k=-\infty}^{\infty} s[k] g\left[k - n_0 \frac{M}{2}\right] e^{-j2\pi m_0 k/M} e^{-j\pi(m_0+n_0)/2}. \tag{2}$$

Therefore, perfect reconstruction of real symbols is performed due to the following real-field orthogonality condition,

$$\Re\left\{\sum_{k=-\infty}^{\infty} g_{m,n}[k] g^*_{m_0,n_0}[k]\right\} = \delta_{m,m_0}\delta_{n,n_0}, \tag{3}$$

where $\delta_{m,m_0} = 1$ if $m = m_0$, and $\delta_{m,m_0} = 0$ if $m \neq m_0$. For simplicity, a interference factor is defined as as

$$\zeta_{m,n}^{m_0,n_0} = \sum_{k=-\infty}^{\infty} g_{m,n}[k] g^*_{m_0,n_0}[k], \tag{4}$$

where $\zeta_{m,n}^{m_0,n_0} = 1$ if $(m, n) = (m_0, n_0)$, and $\zeta_{m,n}^{m_0,n_0}$ is an imaginary value if $(m, n) \neq (m_0, n_0)$. Then, the demodulated signal in (**??**) can be rewritten as

$$\begin{aligned}\hat{a}_{m_0,n_0} &= \sum_{k=-\infty}^{\infty} s[k] g\left[k - n_0 \frac{M}{2}\right] e^{-j2\pi m_0 k/M} e^{-j\pi(m_0+n_0)/2} \\ &= \sum_{k=-\infty}^{\infty} \sum_{m=1}^{M} \sum_{n\in\mathbb{Z}} a_{m,n} g_{m,n}[k] g^*_{m_0,n_0}[k] \\ &= a_{m_0,n_0} + \underbrace{\sum\sum_{(m,n)\neq(m_0,n_0)} a_{m,n}\zeta_{m,n}^{m_0,n_0}}_{i_{m_0,n_0}},\end{aligned} \tag{5}$$

where i_{m_0,n_0} denotes the intrinsic interference term to a_{m_0,n_0} from symbols nearby without considering the channel effects, which is pure imaginary-valued according to the orthogonality conditions in (**??**). In order to recover the transmitted real-valued symbols, the imaginary interference term should be removed, thus an operation of taking real part has to be performed on $\hat{a}_{m,n}$.

B. Single-Tap Equalization in FBMC/OQAM systems

The single-tap equalization plays an important role in symbol demodulation in wireless communications and has been employed in OFDM systems due to the low complexity of implementation. In this subsection, we briefly present the single-tap equalization in FBMC/OQAM under multi-path channels.

Considering a multi-path fading channel with impulse response h of length L_h and complex additive white Gaussian noise (AWGN) $\eta[k]$ with zero mean and variance σ^2. The received signal is written as

$$\begin{aligned} r[k] &= h[k] * s[k] + \eta[k] \\ &= \sum_{l=0}^{L_h-1} h[l] s[k-l] + \eta[k]. \end{aligned} \tag{6}$$

Assume that the maximum delay spread of channel L_h is far less than the length of filterL_g, i.e. $L_h \ll L_g = KM$, so that the prototype function varies slowly within the maximum channel delay spread [**?**]. Then, the demodulated symbols are obtained as

$$\begin{aligned}\hat{a}_{m_0,n_0} =& H_{m_0} a_{m_0,n_0} + \underbrace{\sum\sum_{(m,n)\neq(m_0,n_0)} H_m a_{m,n}\zeta_{m,n}^{m_0,n_0}}_{I_{m_0,n_0}} + \eta_{m_0,n_0} \\ =& H_{m_0}(a_{m_0,n_0} + \sum\sum_{(m,n)\neq(m_0,n_0)} \frac{H_m}{H_{m_0}} a_{m,n}\zeta_{m,n}^{m_0,n_0}) \\ &+ \eta_{m_0,n_0},\end{aligned} \tag{7}$$

where H_m is the channel frequency response with frequency index m, $\eta_{m_0,n_0} = \sum_{k=-\infty}^{\infty} \eta[k] g^*_{m_0,n_0}[k]$ denotes the noise term. Besides, the term I_{m_0,n_0} denotes the total intrinsic interference to the received symbol at time-frequency point (m_0, n_0) considering the channel effects.

To simplify the channel estimation task at the receiver, the channel frequency response in adjacent subcarriers are further assumed to be quasi-invariant, i.e.,

$$H_{m-1} \approx H_m \approx H_{m+1}. \tag{8}$$

Then, the demodulated symbols are simplified as

$$\begin{aligned}\hat{a}_{m_0,n_0} =& H_{m_0}\left(a_{m_0,n_0} + \sum\sum_{(m,n)\neq(m_0,n_0)} a_{m,n}\zeta_{m,n}^{m_0,n_0}\right) + \eta_{m_0,n_0} \\ =& H_{m_0}(a_{m_0,n_0} + i_{m_0,n_0}) + \eta_{m_0,n_0}.\end{aligned} \tag{9}$$

The IAM proposed in [**?**] aims to approximately calculate the imaginary interference term in (**??**) by placing symbols known to the receiver around pilots. Generally, well localized prototype filters are assumed in FBMC/OQAM systems, therefore, only the imaginary interference from $\Omega^*(1, 1)$ is covered in IAM, where $\Omega^*(p, q)$ denotes the neighborhood $\{(m, n) : |m - m_0| \leq p, |n - n_0| \leq q, (m, n) \neq (m_0, n_0).\}$ [**?**], [**?**]. Thus an approximation of the imaginary interference term is obtained in IAM,

$$i_{m_0,n_0} = \sum\sum_{(m,n)\neq(m_0,n_0)} a_{m,n}\zeta_{m,n}^{m_0,n_0} \approx \sum\sum_{\Omega^*(1,1)} a_{m,n}\zeta_{m,n}^{m_0,n_0}. \tag{10}$$

Therefore, the frequency response H_m is estimated in IAM with a pilot inserting at the time-frequency position (m, n) [**?**],

$$\hat{H}_m = \frac{\hat{a}_{m,n}}{a_{m,n} + i_{m,n}} = H_m + \frac{\eta_{m,n}}{a_{m,n} + i_{m,n}}, \tag{11}$$

where $\hat{H}_m$ denotes the estimated value of the channel frequency response. As is indicated in (**??**), it is intrinsic interference term i_{m_0,n_0} along with the noise term η_{m_0,n_0} that accounts for the channel estimation accuracy of IAM.

After the channel response is estimated by the IAM, the single-tap equalization for data symbols can be performed as

$$y_{m_0,n_0} = \frac{\hat{a}_{m_0,n_0}}{H_{m_0}}. \tag{12}$$

Finally, symbols are recovered by taking real part of y_{m_0,n_0} for imaginary interference cancellation.

The single-tap equalization presents good performance under a flat-fading channel. However, severe performance degra-

TABLE I
INTRINSIC INTERFERENCE ONLY TRANSMITTING $a_{m_0,n_0} = 1$ IN FBMC/OQAM

	n_0-3	n_0-2	n_0-1	n_0	n_0+1	n_0+2	n_0+3
m_0-1	ε	δ	γ	β	γ	δ	ε
m_0	θ	0	α	**1**	-α	0	-θ
m_0+1	ε	-δ	γ	-β	γ	-δ	ε

dation would be observed under a frequency-selective channel due to the fact that the assumption in (**??**) is not satisfied well. In the following sections, two channel estimators and an improved C-FBMC/OQAM system are studied by adopting a well-designed repeated frame, respectively. The channel estimators presented in section III focus on the intrinsic interference mitigation for pilots. Moreover, the C-FBMC/OQAM system proposed in sections IV not only focuses on pilots, but also concentrates on the intrinsic interference cancellation for data symbols. It is proven that the proposed schemes can overcome the problem caused by the assumption in (**??**).

III. Repeated Frames Based Channel Estimators Proposed for Intrinsic Interference Cancellation on Pilots in FBMC/OQAM Systems

In this section, the symmetry of intrinsic interference factor is firstly analyzed. Then, two channel estimators with low pilot overheads are demonstrated in FBMC/OQAM systems, in which a repeated frame structure is employed to mitigate the intrinsic interference to pilots. The proposed channel estimators are named as self interference cancellation (SIC) methods, i.e., SIC-1 and SIC-2, respectively.

A. Analysis on Symmetry of Intrinsic Interference Factor

In this subsection, the symmetry of intrinsic interference factor defined in (**??**) is analyzed for symbols on different time-frequency points. Due to the symmetry impulse response of prototype filter as well as the phase rotation employed in FBMC/OQAM, the intrinsic interference from a certain symbol to its surroundings exhibits a symmetry [**?**], [**?**]. Considering a symbol transmitted at (m_0, n_0), the different interference factors to its surroundings are denoted as α, β, γ, δ, θ and ε, respectively, with the magnitudes decreasing progressively. Table **??** illustrates this symmetry of the interference factors, which are expressed as

$$\zeta_{m_0,n_0}^{m_0,n_0-1} = -\zeta_{m_0,n_0}^{m_0,n_0+1} = \alpha, \tag{13}$$

$$\zeta_{m_0,n_0}^{m_0-1,n_0} = -\zeta_{m_0,n_0}^{m_0+1,n_0} = \beta, \tag{14}$$

$$\zeta_{m_0,n_0}^{m_0,n_0-2} = \zeta_{m_0,n_0}^{m_0,n_0+2} = 0, \tag{15}$$

$$\zeta_{m_0,n_0}^{m_0,n_0-3} = -\zeta_{m_0,n_0}^{m_0,n_0+3} = \theta, \tag{16}$$

$$\zeta_{m_0,n_0}^{m_0-1,n_0-1} = \zeta_{m_0,n_0}^{m_0-1,n_0+1} = \zeta_{m_0,n_0}^{m_0+1,n_0-1} = \zeta_{m_0,n_0}^{m_0+1,n_0+1} = \gamma, \tag{17}$$

$$\zeta_{m_0,n_0}^{m_0-1,n_0-2} = \zeta_{m_0,n_0}^{m_0-1,n_0+2} = -\zeta_{m_0,n_0}^{m_0+1,n_0-1} = -\zeta_{m_0,n_0}^{m_0+1,n_0+2} = \delta, \tag{18}$$

$$\zeta_{m_0,n_0}^{m_0-1,n_0-3} = \zeta_{m_0,n_0}^{m_0-1,n_0+3} = \zeta_{m_0,n_0}^{m_0+1,n_0-3} = \zeta_{m_0,n_0}^{m_0+1,n_0+3} = \varepsilon. \tag{19}$$

Furthermore, it is found that, the interference factors exhibit different signs for different time-frequency indexes while the amplitudes remain unchanged. To demonstrate this property, the interference factor $\zeta_{m,n}^{m_0,n_0}$ defined in (**??**) is firstly rewritten as

$$\begin{aligned}\zeta_{m,n}^{m_0,n_0} &= \sum_{k=-\infty}^{\infty} g_{m,n}[k] g_{m_0,n_0}^*[k] \\ &= \sum_{k=-\infty}^{\infty} g\left[k - n\frac{M}{2}\right] g\left[k - n_0\frac{M}{2}\right] \\ &\quad \times e^{j2\pi(m-m_0)k/M} e^{j\pi(m+n-m_0-n_0)/2}.\end{aligned} \tag{20}$$

For simplicity, the ambiguity function is introduced, which is defined as the Fourier transform of the product of the prototype filter response and its conjugate symmetry [**?**],

$$A_g[p\tau, q\upsilon] = \sum_{s=-\infty}^{\infty} g\left[s + \frac{p}{2}\tau\right] g^*\left[s - \frac{p}{2}\tau\right] e^{j2\pi sq\upsilon}, \tag{21}$$

where s is an independent variable, $\tau = M/2$ and $\upsilon = 1/M$ are sampling periods in time and frequency domains, with p, q the corresponding symbol indexes, respectively. Let

$$s + \frac{p}{2}\tau = k - n\frac{M}{2}, \tag{22}$$

$$s - \frac{p}{2}\tau = k - n_0\frac{M}{2}, \tag{23}$$

then the variable s and parameter p are obtained as,

$$s = k - \frac{M(n_0+n)}{4}, \tag{24}$$

$$p = n_0 - n. \tag{25}$$

In addition, to fit the phase term in ambiguity function, parameter q is set as

$$q = m - m_0. \tag{26}$$

Therefore, the interference factor is simplified as equation (**??**). In FBMC/OQAM systems, the prototype filter $g[k]$ is generally real-valued even function [**?**]. Thus, the ambiguity function $A_g\left[(n_0-n)\tau, (m-m_0)\upsilon\right]$ is also real-valued, which denotes the magnitude of the interference factor with its value only depends on the prototype filter response and the relative time-frequency position, i.e., $m_0 - m$ and $n_0 - n$. The phase term $j^{(m-m_0+n-n_0)+(m-m_0)(n+n_0)}$, however, not only depends on the relative position term $m_0 - m$ and $n_0 - n$, but also relies on the absolute time index term $n + n_0$. For a well localized prototype filter, i.e., Phydyas [**?**], IOTA [**?**] , the intrinsic interference to symbols on non-adjacent subcarriers is sufficiently small to be ignored [**?**], [**?**], thus $m - m_0$ only

TABLE II
INTRINSIC INTERFERENCE ONLY TRANSMITTING $a_{m_0,n_0}=1$ IN FBMC/OQAM WITH n_0 **ODD TIME-INDEX** (PHYDYAS, K=4 [**?**])

	n_0-3	n_0-2	n_0-1	n_0	n_0+1	n_0+2	n_0+3
m_0-1	$0.0429j$	$0.1250j$	$0.2058j$	$0.2393j$	$0.2058j$	$0.1250j$	$0.0429j$
m_0	$0.0668j$	0	$0.5644j$	**1**	$-0.5644j$	0	$-0.0668j$
m_0+1	$0.0429j$	-0.1250j	$0.2058j$	-0.2393j	$0.2058j$	-0.1250j	$0.0429j$

TABLE III
INTRINSIC INTERFERENCE ONLY TRANSMITTING $a_{m_0,n_0}=1$ IN FBMC/OQAM WITH n_0 **EVEN TIME-INDEX** (PHYDYAS, K=4 [**?**])

	n_0-3	n_0-2	n_0-1	n_0	n_0+1	n_0+2	n_0+3
m_0-1	$-0.0429j$	$-0.1250j$	$-0.2058j$	$-0.2393j$	$-0.2058j$	$-0.1250j$	$-0.0429j$
m_0	$0.0668j$	0	$0.5644j$	**1**	$-0.5644j$	0	$-0.0668j$
m_0+1	$-0.0429j$	$0.1250j$	$-0.2058j$	$0.2393j$	$-0.2058j$	$0.1250j$	$-0.0429j$

$$\begin{aligned}\zeta_{m,n}^{m_0,n_0} =& \sum_{s=-\infty}^{\infty} g\left[s+\frac{(n_0-n)M/2}{2}\right] g^*\left[s-\frac{(n_0-n)M/2}{2}\right] e^{j2\pi(m-m_0)s/M} e^{j(m-m_0+n-n_0)+(m-m_0)(n+n_0)\pi/2}\\ =&A_g\left[\frac{M(n_0-n)}{2},\frac{m-m_0}{M}\right] e^{[j(m-m_0+n-n_0)+j(m-m_0)(n+n_0)]\pi/2}\\ =&A_g\left[(n_0-n)\tau,(m-m_0)\upsilon\right] j^{(m-m_0+n-n_0)+(m-m_0)(n+n_0)}\end{aligned} \tag{27}$$

takes value of 0 or ± 1.

For the case of $m-m_0=0$, the term $(m-m_0)(n+n_0)$ equals 0, which indicates that the phase of interference factor to symbols on the same subcarrier has no relation to the absolute time index $n+n_0$.

For the other case of $m-m_0=\pm 1$, considering two pairs of symbols with a fixed relative time-frequency index, i.e., (m,n), (m_0,n_0), and $(m,n+b)$, (m_0,n_0+b), where b denotes an integer. The interference factors inner the two pairs are written as

$$\begin{aligned}\zeta_{m_0,n_0}^{m,n} =&A_g\left[(n_0-n)\tau,(m-m_0)\upsilon\right]\\ &\times j^{(m-m_0+n-n_0)+(m-m_0)(n+n_0)},\end{aligned} \tag{28}$$

$$\begin{aligned}\zeta_{m_0,n_0+b}^{m,n+b} =&A_g\left[(n_0-n)\tau,(m-m_0)\upsilon\right]\\ &\times j^{(m-m_0+n-n_0)+(m-m_0)(n+n_0+2b)}.\end{aligned} \tag{29}$$

Thus, the phase rotation between the interference factors is written as

$$\mu=\frac{\zeta_{m_0,n_0+b}^{m,n+b}}{\zeta_{m_0,n_0}^{m,n}}=\frac{j^{(m-m_0)(n+b+n_0+b)}}{j^{(m-m_0)(n+n_0)}}=\begin{cases}-1, & b \text{ is odd,}\\ 1, & b \text{ is even.}\end{cases} \tag{30}$$

It is observed in (**??**) that the phase factors are equal when time indexes n and $n+b$ have the same parity, but have reverse signs when n and $n+b$ have different parities.

The symmetry of interference factor are summarized from the above two cases that symbols with time indexes of different parities exhibits a phase reversal on intrinsic interference for symbols on the adjacent subcarriers, but remains equal for symbols on the current subcarrier. In order to visualize the symmetry illustrated above, Tables **??** and **??** illustrates the interference factors from symbols on odd and even time indexes, respectively, where the typical PHYDYAS prototype filter is employed with overlapping factor set to 4 [**?**].

Owing to the symmetry of interference factor illustrated above, interference cancellation for pilots is valid by means of properly placing symbols on the neighborhood of pilots. In the remainder of this section, two channel estimators are proposed for channel estimation in FBMC/OQAM systems by applying interference cancellation on pilots.

B. SIC-1 Channel Estimator

In this and the next subsections, two channel estimators with low pilot overheads are demonstrated for FBMC/OQAM systems, by employing the repeated frame structures for intrinsic interference cancellation.

The frame structure of SIC-1 is shown in Fig. **??**, where an original frame followed with a repeated frame is included in each block. For simplicity, only 4 subcarriers are displayed, where each sub-frame consists of 7 time indexes according to the OFDM frame structure in long-term evolution (LTE) standard. Note that the data symbols are placed around the pilots without inserting guard symbols to avoid the intrinsic interference to pilots in classic channel estimators like IAM.

As shown in Fig. **??**, in the repeated frame, the data symbols with odd frequency indexes are equal to those in original frame while the pilots have reversed signs, i.e. $a_{m,n}=a_{m,2N+1-n}, P_m^r=-P_m^o$ when m is odd, where N denotes the length of original frame, P_m^o and P_m^r denote the pilots in original and repeated frames, respectively. As for even frequency indexes, the data symbols have opposite signs to original frame while the pilots remains identical.

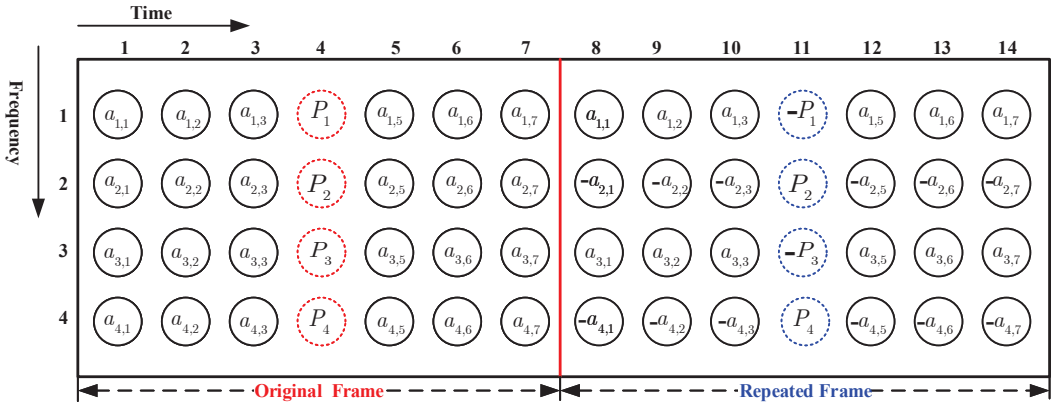

Fig. 2. The frame structure for proposed channel estimator SIC-1.

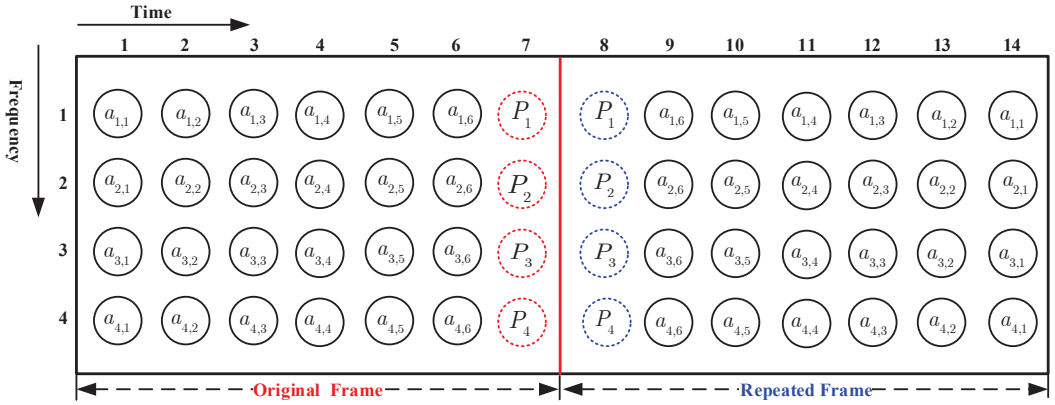

Fig. 3. The frame structure for proposed channel estimator SIC-2.

i.e. $a_{m,n} = -a_{m,2N+1-n}$, $P_m^r = P_m^o$when m is even. The structure illustrated above is designed for interference cancellation to pilots at the subcarriers with odd and even indexes, respectively.

For pilots with odd frequency indexes, taking frequency index at 3 as an example, the intrinsic interference to pilot on the original frame, i.e., $P_3^o = P_3$, is obtained according to (**??**) and the interference factors in Table **??**,

$$\begin{aligned} I_3^o = &\alpha(H_3 * a_{3,5} - H_3 * a_{3,3}) + \theta(H_3 * a_{3,7} - H_3 * a_{3,1}) \\ &+ \beta(H_4 * P_4 - H_2 * P_2) \\ &+ \gamma(H_2 * a_{2,5} + H_2 * a_{2,3} + H_4 * a_{4,5} + H_4 * a_{4,3}) \\ &+ \delta(H_4 * a_{4,6} + H_4 * a_{4,2} - H_4 * a_{2,6} - H_2 * a_{2,2}) \\ &+ \varepsilon(H_4 * a_{4,1} + H_4 * a_{4,7} + H_2 * a_{2,1} + H_2 * a_{2,7}). \end{aligned} \quad (31)$$

Then, the interference to pilot on the repeated frame, i.e., $P_3^r = -P_3$, is written according to the symmetry of interference factor presented in the last subsection,

$$\begin{aligned} I_3^r = &\alpha(H_3 * a_{3,5} - H_3 * a_{3,3}) + \theta(H_3 * a_{3,7} - H_3 * a_{3,1}) \\ &- \beta(H_4 * P_4 - H_2 * P_2) \\ &- \gamma(H_2 * -a_{2,5} - H_2 * a_{2,3} - H_4 * a_{4,5} - H_4 * a_{4,3}) \\ &- \delta[H_4 * -a_{4,6} - H_4 * a_{4,2} - H_2(-a_{2,6}) - H_2(-a_{2,2})] \\ &- \varepsilon(H_4 * -a_{4,1} - H_4 * a_{4,7} - H_2 * a_{2,1} - H_2 * a_{2,7}). \end{aligned} \quad (32)$$

It is easily to observe that interference from data symbols is equal for P_3^r and P_3^o, which can be removed by means of a subtracting operation,

$$I_3^o - I_3^r = 2\beta * (H_4 P_4 - H_2 P_2). \quad (33)$$

Therefore, the received symbols with respect to both pilots can be obtained,

$$r_3^o = H_3^o * P_3 + I_3^o + \eta_3^o, \quad (34)$$

$$r_3^r = H_3^r(-P_3) + I_3^r + \eta_3^r. \quad (35)$$

where H_3^o and H_3^r denote channel frequency response, which is assumed to satisfy the frequency quasi-invariant condition in (**??**) and be quasi-invariant within the subframe for each subcarrier, i.e., $H_m = H_m^o = H_m^r$. Finally, the channel frequency response are estimated by a subtracting operation,

$$r_3^o - r_3^r = 2H_3 P_3 + \eta_3^o - \eta_3^r + 2\beta(H_4 P_4 - H_2 P_2), \quad (36)$$

$$\hat{H}_3 = \frac{r_3^o - r_3^r}{2P_3 + 2\beta(P_4 - P_2)} = H_3 + \frac{\eta_3^o - \eta_3^r}{2P_3 + 2\beta(P_4 - P_2)}. \quad (37)$$

where $\hat{H}_3$ represents the estimated value of the channel frequency response H_3.

As for pilots with even frequency index, similarly, interference from data symbols for both pilots has equal amplitude but with opposite signs, which can be removed by means of an adding operation, taking the P_2^o and P_2^r pilots pair as an example,

$$I_2^o + I_2^r = 2\beta(H_3P_3 - H_1P_1), \tag{38}$$

therefore, the channel frequency response are estimated by an adding combination,

$$r_2^o + r_2^r = 2H_2P_2 + \eta_2^o + \eta_2^r + \beta(H_3P_3 - H_1P_1), \tag{39}$$

$$\hat{H}_2 = \frac{r_2^o + r_2^r}{2P_2 - 2\beta(P_3 - P_1)} = H_2 + \frac{\eta_2^o + \eta_2^r}{2P_2 - 2\beta(P_3 - P_1)}. \tag{40}$$

Conclusion can be drawn from the above analyses that the intrinsic interference from data symbols to pilots are radically mitigated and the pilot overheads are reduced to two columns of real-valued pilots in SIC-1.

C. SIC-2 Channel Estimator

Compared with conventional IAM, the pilot overhead is reduced in SIC-1. However, the proposed SIC-1 still relies on the quasi-invariant channel frequency response assumption. In this subsection, a new scheme SIC-2 for interference cancellation on pilots is proposed, which breaks the limits of assumption in (**??**). Compared to SIC-1, intrinsic interference can be eliminated more thoroughly in SIC-2 that the intrinsic interference from pilots on adjacent subcarriers are also mitigated.

Fig. **??** depicts the frame structure of SIC-2, which is similar to that of SIC-1 in a whole view except that data symbols in the repeated frame are transmitted in reverse order, i.e. $a_{m,n} = a_{m,2N+1-n}$ and the identical pilots are located on the end of the original frame as well as the beginning of the repeated frame, i.e. $P_m = P_m^o = P_m^r$, respectively. Similar to SIC-1, here N denotes the length of original frame, P_m^o and P_m^r denote the pilots in original and repeated frames, respectively. It is worthy of noting that the similar time-reversal technique is also employed in different transmitting antennas in (**?**) to maintain the orthogonality of Alamouti at the receiver. The main difference lies that intrinsic interference is not mitigated in (**?**), therefore guard symbols and the operation of taking real part are still necessary. In the proposed SIC-2 and C-FBMC/OQAM in next section, the intrinsic interference are radically canceled so that guard symbols and the operation of taking real part are not required, as you can see from the analysis below.

For pilot P_m^o in the original frame, the interference suffered from adjacent pilots and data symbols is written according to Table **??**,

$$\begin{aligned} I_m^o = {} & \alpha * H_m(P_m - a_{m,6}) + \theta * H_m(a_{m,5} - a_{3,4}) \\ & + \beta * (H_{m+1}P_{m+1} - H_{m-1}P_{m-1}) \\ & + \gamma * (H_{m-1}a_{m-1,6} + H_{m+1}a_{m+1,6}) \\ & + \gamma * (H_{m-1}P_{m-1} + H_{m+1}P_{m+1}) \\ & + \delta * (H_{m+1}a_{m+1,6} + H_{m+1}a_{m+1,5}) \\ & - \delta * (H_{m-1}a_{m-1,6} + H_{m-1}a_{m-1,5}) \\ & + \varepsilon * (H_{m+1}a_{m+1,4} + H_{m+1}a_{m+1,5}) \\ & + \varepsilon * (H_{m-1}a_{m-1,4} + H_{m-1}a_{m-1,5}), \end{aligned} \tag{41}$$

Then, the intrinsic interference to pilots on the repeated frame is obtained according to the symmetry of interference factor,

$$\begin{aligned} I_m^r = {} & \alpha * H_m(a_{m,6} - P_m) + \theta * H_m(a_{3,4} - a_{m,5}) \\ & - \beta * (H_{m+1}P_{m+1} - H_{m-1}P_{m-1}) \\ & - \gamma * (H_{m-1}P_{m-1} + H_{m+1}) \\ & - \gamma * (P_{m+1} + a_{m-1,6} + a_{m+1,6}) \\ & - \delta * (H_{m+1}a_{m+1,6} + H_{m+1}a_{m+1,5}) \\ & - (-\delta) * (H_{m-1}a_{m-1,6} + H_{m-1}a_{m-1,5}) \\ & - \varepsilon * (H_{m+1}a_{m+1,4} + H_{m+1}a_{m+1,5}) \\ & - \varepsilon * (H_{m-1}a_{m-1,4} + H_{m-1}a_{m-1,5}), \end{aligned} \tag{42}$$

It can be easily observed from (**??**) and (**??**) that the interference are completely canceled by an adding combination,

$$I_m^o + I_m^r = 0 \tag{43}$$

Therefore, the received symbols with respect to the pilots are obtained as

$$r_m^o = H_m^o P_m + I_m^o + \eta_m^o, \tag{44}$$

$$r_m^r = H_m^r P_m + I_m^r + \eta_m^r, \tag{45}$$

Similarly, the channel frequency response is assumed to be time quasi-invariant within a subframe, i.e., $H_m = H_m^o = H_m^r$. Finally, the channel frequency response are estimated by a linear summation,

$$\hat{H}_m = \frac{r_m^o + r_m^r}{2P_m} = H_m + \frac{\eta_m^o + \eta_m^r}{2P_m}. \tag{46}$$

As analyzed above, the proposed SIC-2 achieves a thorough interference cancellation among adjacent subcarriers for pilots, with pilot overhead also one column per frame. The pilots can also be randomly picked real numbers and the extra pseudo power gain is zero here since the interference from adjacent pilots is removed. Therefore, the differences between the proposed SIC-1 and SIC-2 are concluded as follows:

- SIC-2 radically removes the intrinsic interference to pilots, however, the intrinsic interference to pilots from adjacent pilots are remained in SIC-1, which act as a pseudo pilot as in IAM.
- In SIC-2, the pilots can be randomly selected, however, the pilot sequence should be design as IAM in SIC-1 to get an extra pseudo power gain, which present a promotion in the accuracy of channel estimation but results in higher peak to average power ratio (PAPR) as well.
- In SIC-1, the intrinsic interference on data symbols can not be removed, however, in SIC-2, it is interesting to find that the interference to data symbols can also be mitigated by means of the same summation operations performed on pilots in SIC-2, which enables the proposal of C-FBMC/OQAM in the next section.

As a remark, since the symbol repetition in SIC-1 and SIC-2 will reduce the spectral efficiency, the C-FBMC/OQAM is proposed in Sec. IV to maintain the spectral efficiency, in which

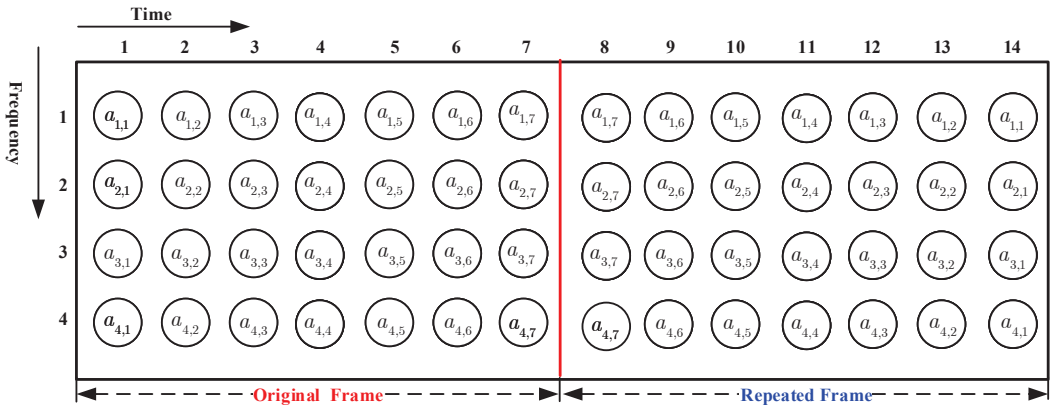

Fig. 4. The frame structure for C-FBMC/OQAM system.

$$\sum_{k=-\infty}^{\infty} g_{m,n}[k]g^*_{m_0,n_0}[k] = \sum_{k=-\infty}^{\infty} g[k-nM/2]g[k-n_0M/2]e^{j2k\pi(m-m_0)/M}e^{j\pi(m+n-m_0-n_0)/2},$$
$$= \sum_{w=-\infty}^{\infty} g[w]g[w+(n-n_0)M/2]e^{jn\pi(m-m_0)}e^{j2\pi w(m-m_0)/M}e^{j\pi(m+n-m_0-n_0)/2}. \quad (47)$$

complex-valued symbols are transmitted instead of real-valued symbols. Besides, different from the classic FBMC/OQAM, the assumption on **??**, i.e., $H_{m-1} \approx H_m \approx H_m + 1$, is not required for both of data and pilot symbols in the proposed C-FBMC/OQAM.

IV. Repeated Frames Based C-FBMC/OQAM System Proposed for Intrinsic Interference Cancellation.

In section III, two frame structures are proposed for channel estimation in classic FBMC/OQAM system based on interference cancellation, and particularly a thorough interference elimination for pilots is achieved in SIC-2. In this section, we focus on intrinsic interference cancellation among data symbols, and a novel C-FBMC/OQAM system adopting a well-design frame structure is illustrated, followed with performance analysis of C-FBMC/OQAM systems. Instead of dividing complex QAM symbols into real and imaginary parts in FBMC/OQAM systems, the proposed C-FBMC/OQAM system separate each QAM symbol into two identical symbols with half power, which are transmitted in the original and repeated frames, respectively. The length of each symbol is the same as that of FBMC/OQAM symbols due to a decreased power, therefore the total time for data transmission is the same as FBMC/OQAM and OFDM systems. At the receiver, combination operations are performed as SIC-2 to eliminate the intrinsic interference for both pilots and data symbols.

A. System Structure of C-FBMC/OQAM

In this subsection, we firstly design the complete frame structure of C-FBMC/OQAM according to the feature of Table. **??** and Table. **??**, consisting of a original frame and a repeated frame as shown in Fig. **??**, and then provide the orthogonality condition of C-FBMC/OQAM, explaining why complex-valued symbols can be transmitted instead of only real-valued symbols in the classic FBMC/OQAM.

From Table. **??** and Table. **??**, the symmetry of interference factor is observed, i.e., symbols with odd and even indexes exhibits a phase reversal on intrinsic interference for symbols on the adjacent subcarriers, while remains equal for symbols on the current subcarrier. On this basis, the structures of original and repeated frames are presented so that the following orthogonality condition can be satisfied, achieving the imaginary interference cancellation for both of the pilot and data symbols. Assume that the length of original frame is N, $a_{m,n}$ is data symbol at the time-frequency position (m,n) with $n \in [1, 2N]$. The intrinsic interference factor presented in (**??**) is rewritten in (**??**) for C-FBMC/OQAM system, where $w = k - nM/2$. Note that the term $e^{jn\pi(m-m_0)}$ has opposite signs for symbols with odd and even time indexes, which accords with the symmetry of intrinsic interference factor demonstrated in Sec.III. Therefore, the following orthogonality condition of the proposed C-FBMC/OQAM holds,

$$\sum_{k=-\infty}^{\infty} g_{m,n}[k]g^*_{m_0,n_0}[k] + \sum_{k=-\infty}^{\infty} g_{m,2N+1-n}[k]g^*_{m_0,2N-n_0}[k]$$
$$= 2\delta_{m,m_0}\delta_{n,n_0}. \quad (48)$$

Note that $g_{m,n}[k]$ is defined in (**??**). Based on the orthogonality condition, it is easily derived that the imaginary interference will vanish if one symbol is placed at the time-frequency (m,n) in the original frame and $(m, 2N-n)$ in the repeated frame, i.e., $a_m, n = a_m, 2N+1-n$. Therefore, the transmitted

symbols $a_{m,n}$ can be complex-valued, instead of only real-valued in the classic FBMC/OQAM.

For simplicity, assume that $a^o_{m,n} = a_{m,n}$ is the symbols in the original frame and $a^r_{m,n} = a_{m,2N+1-n}$ is the symbols in the repeated frame. Then, the demodulated symbols at the receiver can be obtained according to (**??**),

$$r^o_{m_0,n_0} = H_{m_0} a^o_{m_0,n_0} + \underbrace{\sum_{(m,n)\neq(m_0,n_0)} \sum H_m a^o_{m,n} \zeta^{m_0,n_0}_{m,n}}_{I^o_{m,n}} + \eta^o_{m_0,n_0}, \tag{49}$$

$$r^r_{m_0,n_0} = H_{m_0} a^r_{m_0,n_0} + \underbrace{\sum_{(m,n)\neq(m_0,n_0)} \sum H_m a^r_{m,n} \zeta^{m_0,2N+1-n_0}_{m,2N+1-n}}_{I^r_{m,n}} + \eta^r_{m_0,n_0}. \tag{50}$$

Note that, noises $\eta^o_{m_0,n_0}$ and $\eta^r_{m_0,n_0}$ can be obtained according to (**??**), satisfying Gaussian distribution with mean 0 and variance σ^2. Then, for the interference terms $I^o_{m,n}$, $I^r_{m,n}$, it is obtained according to the orthogonality condition in (**??**),

$$\begin{aligned} I^o_{m,n} + I^r_{m,n} = & \sum_{(m,n)\neq(m_0,n_0)} \sum H_m a^o_{m,n} \zeta^{m_0,n_0}_{m,n} \\ & + \sum_{(m,n)\neq(m_0,n_0)} \sum H_m a^r_{m,n} \zeta^{m_0,2N+1-n_0}_{m,2N+1-n}, \\ = & \, 0. \end{aligned} \tag{51}$$

It is worthwhile to note that, in (**??**), the assumption on a flat fading channel is relaxed since the assumption in (**??**), i.e., $H_{m-1} \approx H_m \approx H_{m+1}$, is not required yet. However, the above assumption is necessary for the classic FBMC/OQAM to enable the single-tap channel equalization. Therefore, the proposed C-FBMC/OQAM exhibits advantages over the classic FBMC/OQAM under frequency-selective channels, which will be verified in simulation results.

Taking symbol $a_{2,4}$ for example, in the original frame, the interference is written as

$$\begin{aligned} I^o_{2,4} = & \alpha * H_2 * (a_{2,5} - a_{2,3}) + \theta * H_2 * (a_{2,7} - a_{2,1}) \\ & + \beta(H_3 * P_3 - H_1 * P_1) \\ & + \gamma(H_1 * a_{1,5} + H_1 * a_{1,3} + H_3 * a_{3,5} + H_3 * a_{3,3}) \\ & + \delta(H_3 * a_{3,6} + H_3 * a_{3,2} - H_1 * a_{1,6} - H_1 * a_{1,2}) \\ & + \varepsilon(H_3 * a_{3,1} + H_3 * a_{3,7} + H_1 * a_{1,1} + H_1 * a_{1,7}). \end{aligned} \tag{52}$$

In the repeated frame, the corresponding interference is

$$\begin{aligned} I^r_{2,4} = & \alpha * H_2 * (a_{2,3} - a_{2,5}) + \theta * H_2 * (a_{2,1} - a_{2,7}) \\ & - \beta(H_3 * P_3 - H_1 * P_1) \\ & + \gamma(H_1 * a_{1,3} + H_1 * a_{1,5} + H_3 * a_{3,3} + H_3 * a_{3,5}) \\ & - \delta(H_3 * a_{3,2} + H_3 * a_{3,6} - H_1 * a_{1,2} - H_1 * a_{1,6}) \\ & - \varepsilon(H_3 * a_{3,7} + H_3 * a_{3,1} + H_1 * a_{1,7} + H_1 * a_{1,1}). \end{aligned} \tag{53}$$

It's evident that $I^o_{m,n} + I^r_{m,n} = 0$ holds for $a_{2,4}$ pair even if the assumption in (**??**) does not hold any longer. The $I^o_{m,n} + I^r_{m,n} = 0$, likewise, holds for all data symbol pairs as long as the symmetry is satisfied, which indicates that the performance of C-FBMC/OQAM would be improved under frequency selective channels compared with the conventional FBMC/OQAM systems.

Based the theoretical analyses above, the C-FBMC/OQAM system is put forward with frame structure depicted in Fig. **??**, where all the symbols transmitted are complex-valued. Meanwhile, in order to settle the problem that the interference at the frame edge cannot be eliminated due to data asymmetry between frame blocks, the edge of the frame block (the first column symbols in original frame and the last column symbols in the repeated frame) is reserved for pilots. Placing the randomly chosen pilots at the edge columns in each frame block, the interference cancellation for frame margin can be achieved, and the channel frequency response can be estimated as SIC-2 does.

At the receiver, the intrinsic interference can be easily eliminated by an adding combination,

$$\begin{aligned} r_{m,n} &= (r^o_{m,n} + r^r_{m,n})/2 \\ &= H_m a_{m,n} + (\eta^o_{m,n} + \eta^r_{m,n})/2, \end{aligned} \tag{54}$$

then the symbols can be recovered with the aid of the estimated channel frequency response,

$$\begin{aligned} \hat{a}_{m,n} &= r_{m,n}/H_m \\ &= a_{m,n} + (\eta^o_{m,n} + \eta^r_{m,n})/(2H_m). \end{aligned} \tag{55}$$

The derivation above reveals that the mutual intrinsic interference among data symbols is eliminated and the data transmitted can be perfectly recovered with the estimated channel frequency response in C-FBMC/OQAM system.

The equivalent baseband block diagram of C-FBMC/OQAM system is shown in Fig **??**, where the well-designed frame block is complied with a order-reversed repeated frame following the original frame in the transmitter and symbols are recovered from adding combinations and easy-implemented equalizations at the receiver. Besides, it is worthwhile to note that guard symbols are not necessary to separate frames since pilot symbols are placed at the beginning of the original frames and at the end of the repeated frames. The pilot symbols are employed only for channel estimation but also acted as guard symbols to suppress the interference to symbols at the edge of frame from neighborhood frames.

B. Performance Analysis of C-FBMC/OQAM systems

The performance analysis on C-FBMC/OQAM systems is presented in this subsection in terms of spectral efficiency and OOB emission, compared with conventional FBMC/OQAM and OFDM systems. It is proven that, the proposed C-FBMC/OQAM systems retain high spectral efficiency as in FBMC/OQAM systems, even in the existence of a repeated frame.

Firstly, the spectral efficiency of C-FBMC/OQAM system is derived based on an AWGN channel with noise power σ^2. To ensure a fair comparison, the total signal power is supposed to be the same. We denote the power of an OFDM symbol as p_s. Then, a complete complex symbol, including real part and imaginary part, has a power of p_s in FBMC/OQAM systems. In C-FBMC/OQAM systems, each symbol is supposed to have a half power $p_s/2$ to maintain an identical total signal power in the existence of a repeated frame.

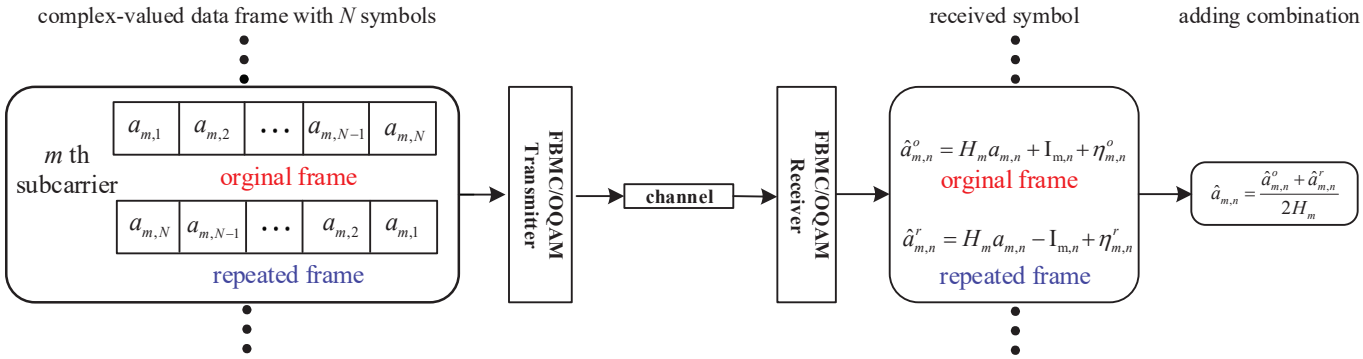

Fig. 5. The equivalent baseband block diagram of C-FBMC/OQAM system.

The spectral efficiency is defined as channel capacity normalized by bandwidth, obtained as

$$C = \log_2(1+R) \quad (bit/s/Hz), \tag{56}$$

where R denotes the receiving signal to noise ratio(SNR).

In OFDM systems, the SNR can be easily obtained as,

$$R_{OFDM} = \frac{p_s}{\sigma^2}. \tag{57}$$

In FBMC/OQAM systems, complex-valued symbols are partitioned into real and imaginary parts and transmitted as a pair of real-valued symbols. The received symbols are contaminated by imaginary interference,

$$r_{m,2k} = a_{m,2k} + I_{m,2k} + \eta_{m,2k}, \tag{58}$$

$$r_{m,2k+1} = a_{m,2k+1} + I_{m,2k+1} + \eta_{m,2k+1}, \tag{59}$$

The transmitted symbols are recovered by taking the real parts of the received symbols,

$$\hat{a}_{m,2k} = \Re(r_{m,2k}) = a_{m,2k} + \Re(\eta_{m,2k}), \tag{60}$$

$$\hat{a}_{m,2k+1} = \Re(r_{m,2k+1}) = a_{m,2k+1} + \Re(\eta_{m,2k+1}). \tag{61}$$

Then, the complex symbol is retrieved as,

$$\begin{aligned}\hat{a}_{m,n} &= \hat{a}_{m,2k} + j\hat{a}_{m,2k+1}, \\ &= a_{m,2k} + ja_{m,2k+1} + \Re(\eta_{m,2k}) + j\Re(\eta_{m,2k+1}).\end{aligned} \tag{62}$$

Therefore, the SNR is obtained as,

$$R_{FBMC/OQAM} = \frac{|a_{m,2k} + ja_{m,2k+1}|^2}{|\Re(\eta_{m,2k}) + j\Re(\eta_{m,2k+1})|^2}. \tag{63}$$

where $a_{m,2k}$ and $a_{m,2k+1}$ are combined into a complete complex symbol with power p_s. Besides, $\eta_{m,2k}$ and $\eta_{m,2k+1}$ are complex white Gaussian noise, in which the real and imaginary parts take up half power, respectively. Therefore, the total power of noise term is also σ^2. Then (**??**) can be written as,

$$R_{FBMC/OQAM} = \frac{p_s}{\sigma^2}. \tag{64}$$

In the proposed C-FBMC/OQAM, each complex-valued symbol is transmitted twice in the original and repeated frames with half power compare to OFDM symbols. The original and repeated symbols suffer equal intrinsic interference with opposite signs. The received symbols are obtained as,

$$\hat{a}^o_{m,n} = a_{m,n} + I_{m,n} + \eta^o_{m,n}, \tag{65}$$

$$\hat{a}^r_{m,n} = a_{m,n} - I_{m,n} + \eta^r_{m,n}. \tag{66}$$

Then, symbols are recovered by an adding combination,

$$\begin{aligned}a_{m,n} =& \frac{\hat{a}^o_{m,n} + \hat{a}^r_{m,n}}{2}, \\ =& a_{m,n} + \frac{\eta^o_{m,n} + \eta^r_{m,n}}{2}.\end{aligned} \tag{67}$$

Therefore, the SNR of C-FBMC/OQAM systems is obtained as,

$$R_{C-FBMC/OQAM} = \frac{|a_{m,n}|^2}{\left|(\eta^o_{m,n} + \eta^r_{m,n})/2\right|^2}, \tag{68}$$

where $a_{m,n}$ takes up half power as OFDM symbols, i.e., $p_s/2$. Besides, $\eta^o_{m,n}$ and $\eta^r_{m,n}$ are independent and identically distributed (i.i.d) Gaussian noise with mean zero and variance σ^2, then the total power of noise term is $\sigma^2/2$. Therefore,

$$R_{C-FBMC/OQAM} = \frac{p_s/2}{\sigma^2/2} = \frac{p_s}{\sigma^2}. \tag{69}$$

The analysis above demonstrates that the receiving SNR is equal for OFDM, FBMC/OQAM and C-FBMC/OQAM systems. Therefore, the spectral efficiency performance of C-FBMC/OQAM system keeps the same as that of OFDM and FBMC/OQAM systems without considering extra consumption of CP and pilots.

Taking account of CP and pilot overheads for channel estimation, OFDM system requires a column of complex pilot symbols per frame for channel estimation and CP is introduced to against multi-path fading channels. FBMC/OQAM system needs three columns of real-valued pilot symbols (equivalent to 1.5 columns of complex symbols) for channel estimation. C-FBMC/OQAM system demands one columns of complex symbols for channel estimation. In this way, the proposed C-FBMC/OQAM system presents lower extra consumption of resources compared to OFDM with CP and FBMC/OQAM systems, which leads to a higher spectral efficiency. It is worth noting that the symbols separation in C-FBMC/OQAM

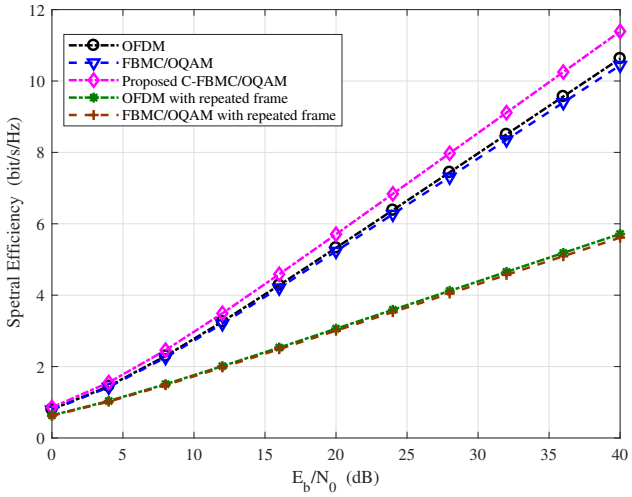

Fig. 6. Spectral efficiency performances for the OFDM, FBMC/OQAM, and proposed C-FBMC/QAM systems considering CP and pilot overheads.

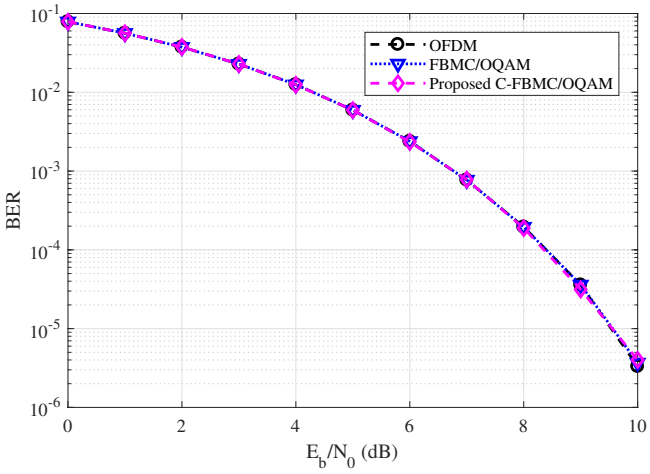

Fig. 7. BER performances for the OFDM, FBMC/OQAM, and proposed C-FBMC/OQAM systems under AWGN channel.

could also be performed in OFDM systems even if it does not provide performance improvements. As for directly repeating a data frame in OFDM or FBMC/OQAM system, a better transmission reliability could be achieved with a decreased spectral efficiency in exchange.

In Fig. **??**, the proposed C-FBMC/OQAM system is compared with OFDM, FBMC/OQAM systems and their direct-repeated versions in terms of spectral efficiency to validate our analyses, in which the CP and pilot overheads are considered (Note that, only block-type pilots are considered). Generally, the frame repetition is not employed in the classic OFDM and FBMC/OQAM systems, since the frame repetition will reduce the spectral efficiency greatly. In this paper, the QAM symbols are partitioned into two identical parts and transmitted in the original and repeated frames with half of symbol interval as that of OFDM, so that the spectral efficiency is maintained. Besides, the normal mode of LTE frame structure is employed for evaluation, where each slot consists of 7 OFDM symbols with effective symbol time 66.7 μs, the first symbol has a CP of length 5.2 μs and the remaining six symbols have a CP of length $4.7\mu s$ [**?**]. The simulation result accords with the analyses above that the proposed C-FBMC/OQAM system slightly outperforms conventional OFDM with CP and FBMC/OQAM systems in terms of spectral efficiency performance due to the fact that C-FBMC/OQAM does not require CP and the pilot overheads are equal to that of OFDM.

As for the OOB performance, the proposed C-FBMC/OQAM system does not make any changes to the prototype filters, so that the well-localization and low OOB emission properties in FBMC/OQAM system are maintained. However, in FBMC/QAM system, the changes to prototype filters results in severe decrease in localization and OOB performance.

Conclusions can be drawn from the above comparisons that the proposed C-FBMC/OQAM systems radically mitigate intrinsic interference without sacrificing spectral efficiency and OOB emission performance.

V. Simulation Results

In this section, simulation results are presented to verify the performance of the proposed C-FBMC/OQAM systems and channel estimators SIC-1 and SIC-2 in terms of BER and MSE. The simulations are carried out under AWGN channel and multi-path fading channel models SUI-1, SUI-3 and SUI-4 [**?**], respectively. The channel profiles are shown in Table **??** [**?**], which indicates that the frequency selectivity gets higher from SUI-1 to SUI-4. In order for impartial evaluation of performance, pilot column used for channel frequency response estimation keeps identical in each channel estimators, the randomly generated ± 1 sequence is adopted in our simulation. Detailed parameters for simulations are listed as follows.

- Sampling rate: 30.72 MHz
- Subcarriers number: $M = 2048$
- Modulation: 4QAM
- Channel coding: no
- Length of CP in OFDM: $M/8 = 256$ samples
- Prototype filter: PHYDYAS
- Overlapping factor: $K = 4$
- Frame length: 7 QAM symbols in each frame

A. AWGN channel

Fig. **??** depicts the BER performances for the OFDM, conventional FBMC/OQAM, and proposed C-FBMC/QAM systems under AWGN channel. The simulation results validate that the proposed C-FBMC/OQAM system presents the same BER performance under AWGN channel compared to conventional FBMC/OQAM and OFDM systems. The reasons are summarized as two aspects in the following. Firstly, due to the symmetry of interference factor, symbols in the original frame and repeated frame have opposite intrinsic interference, which is completely mitigated by adding combinations. Thus, the proposed C-FBMC/QAM systems are interference-free for transmitting complex QAM symbols. Besides, the receiving SNR is proven to be equal in AWGN channel in section IV,

TABLE IV
PROFILES OF SUI-1, SUI-3 AND SUI-4 CHANNEL MODEL [**?**]

Channel	SUI-1	SUI-3	SUI-4
Number of Paths	3	3	3
Power Profile (in dB)	0,-15.0,-20.0	0,-5.0,-10.0	0,-4.0 -8.0
Delay Profile(μs)	0,0.4,0.9	0,0.4,0.9	0,1.5,4.0

which indicates that the theoretical value of BER are equal for OFDM, FBMC/OQAM and C-FBMC/OQAM systems. Therefore, the proposed C-FBMC/QAM system demonstrates the same BER performances as the OFDM and conventional FBMC-OQAM systems in AWGN channel.

B. SUI-1 channel model

Figs. **??** and **??** present the MSE and BER performance for the OFDM, FBMC/OQAM, the proposed C-FBMC/OQAM and channel estimators under SUI-1 channel, respectively. From the MSE results, in the overall view, only IAM in FBMC/OQAM presents performance floor while other estimators exhibit near linear MSE curves in the SNR range, due to the remaining intrinsic interference in FBMC/OQAM system and the sensitivity of IAM to channel frequency selectivity. Observing from different parts, the proposed SIC-1 and conventional IAM outperform OFDM, SIC-2 and C-FBMC/OQAM at low SNR range 0-5 dB. The reason goes that the intrinsic interference from adjacent pilots remained in the former two channel estimators turns into part of the pseudo-pilot, offering a suppression on the power of noise component and a promotion in the accuracy of channel estimation. At middle SNR range, the MSE of IAM gradually bends, SIC-1 still exhibits slightly advantage over OFDM, SIC-2 and C-FBMC/OQAM. When it goes to high SNR over about 30 dB, OFDM provides superior performance over other channel estimator owing to its robustness to channel frequency selectivity with the insertion of CP. The BER results accord with the analysis above, which SIC-1 and IAM have advantage over other estimators in low SNR range while suffering a performance loss in the high SNR range, and OFDM slightly outperform C-FBMC/OQAM and SIC-2.

C. SUI-3 channel model

Figs. **??** and **??** depict the MSE and BER performance for the OFDM, FBMC/OQAM, the proposed C-FBMC/OQAM and channel estimators under SUI-3 channel, respectively. Similar to SUI-1 case, SIC-1 and IAM outperforms other estimators in low SNR range due to the suppression on noise component brought from pseudo-pilot, and OFDM illustrates a superior performance in the high SNR range because of its validity under frequency selective channels. The main differences with the SUI-1 circumstance are outlined as the following two points. Firstly, the BER performance of IAM, C-FBMC/OQAM, SIC-1 and SIC-2 suffer slight declines as a consequence of the intenser frequency selectivity of SUI-3 channel compared to SUI-1. Correspondingly, the MSE performance of them exhibits visible bending in the high SNR

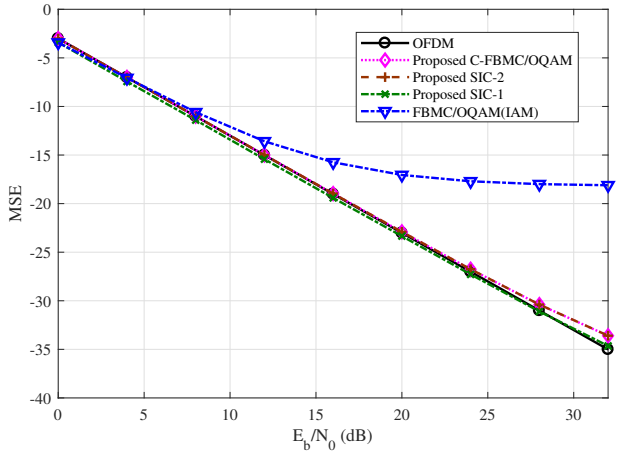

Fig. 8. MSE performance for the OFDM, FBMC/OQAM, proposed C-FBMC/OQAM and channel estimators under SUI-1 channel.

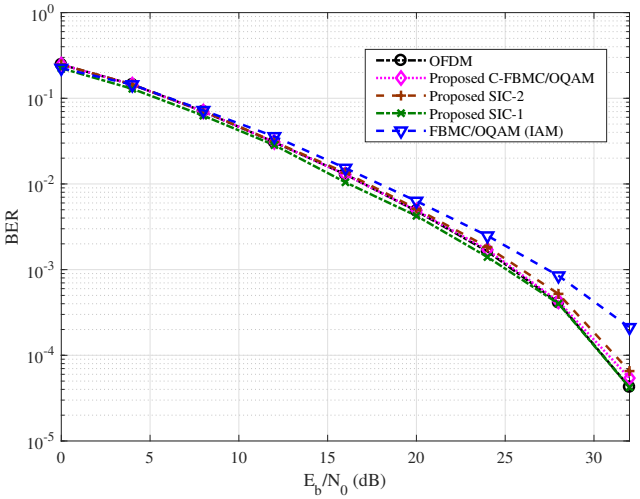

Fig. 9. BER performance for the OFDM, FBMC/OQAM, proposed C-FBMC/OQAM and channel estimators under SUI-1 channel.

range over about 25 dB. Besides, the BER performance of SUI-1 is inferior to that of OFDM in the high SNR range over 28 dB, which indicates that the benefit from pseudo-pilot is not enough to compensate the loss caused by channel frequency selectivity. Meanwhile, the BER performance of SUI-1 is still superior to that of C-FBMC/OQAM, demonstrating that under SUI-3 channel, the channel estimation gain from pseudo-pilot is superior to the increased robustness to channel frequency selectivity of C-FBMC/OQAM to SIC-1 from the intrinsic

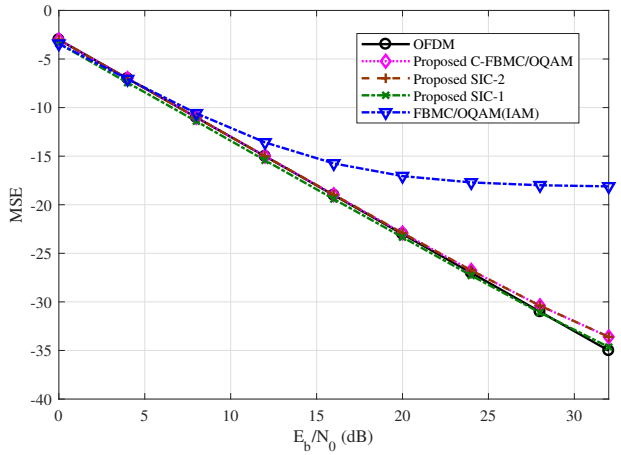

Fig. 10. MSE performance for the OFDM, FBMC/OQAM, proposed C-FBMC/OQAM and channel estimators under SUI-3 channel.

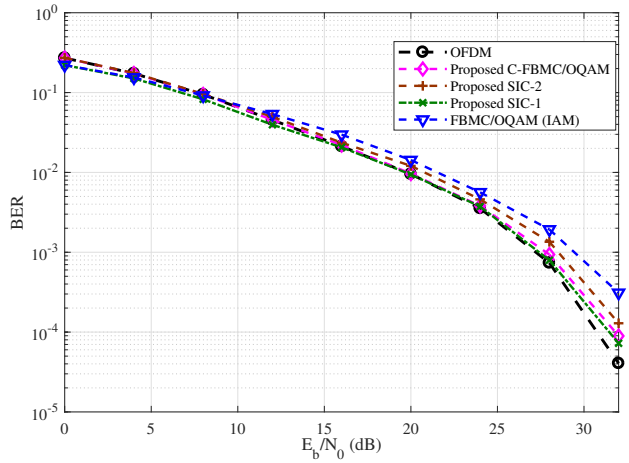

Fig. 11. BER performance for the OFDM, FBMC/OQAM, proposed C-FBMC/OQAM and channel estimators under SUI-3 channel.

interference cancellation of data symbols.

D. SUI-4 channel model

Figs. **??** and **??** illustrate the MSE and BER performance of the proposed C-FBMC/OQAM system under SUI-4 channel, respectively. It is interesting to observe that, although the proposed SIC-1 and SCI-2 schemes exhibit better MSE performance than the proposed C-FBMC/OQAM scheme, the BER performance of the C-FBMC/OQAM systems is better than the SIC-1, SIC-2 and the classical FBMC/OQAM systems. The BER performance gain can be observed obviously for both of the low SNR range and the high SNR range. The reason is that, the proposed C-FBMC/OQAM system can eliminate the interference completely caused by the assumption in (**??**), i.e., the imaginary interferences in the original and repeated frames hold $I^o_{m,n} + I^r_{m,n} = 0$ as you can see (**??**) and (**??**) in section IV.

As a remark, under channels with very high frequency selectivity, the proposed C-FBMC/OQAM systems still suffer

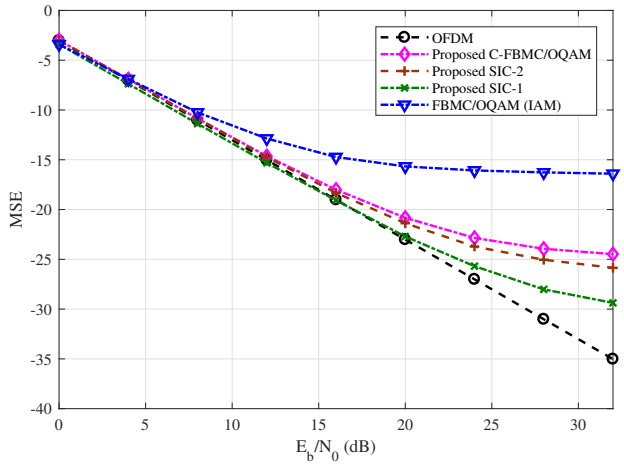

Fig. 12. MSE performance for the OFDM, FBMC/OQAM, proposed C-FBMC/OQAM and channel estimators under SUI-4 channel.

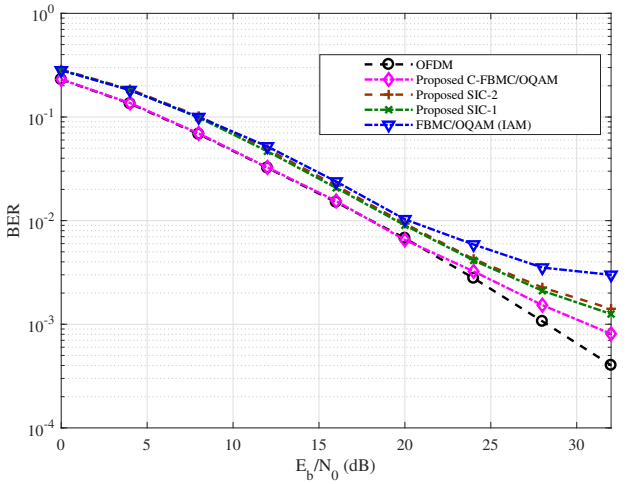

Fig. 13. BER performance for the OFDM, FBMC/OQAM, proposed C-FBMC/OQAM and channel estimators under SUI-4 channel.

some performance loss compared with OFDM systems with CP since the assumption on channel maximum delay in (**??**) does not holds any longer. Therefore, as a future work, it will be interesting to investigate the C-FBMC/OQAM system under channels with high frequency selectivity.

VI. Conclusion

In this paper, we concentrate on the intrinsic interference elimination in FBMC/OQAM systems. A novel FBMC/OQAM system called C-FBMC/OQAM was proposed that radically eliminate the intrinsic interference for both data symbols and pilots without sacrificing spectral efficiency and OOB performance. Besides, two pilot-aided channel estimators SIC-1 and SIC-2 were put forward for FBMC/OQAM systems with 2/3 pilot overheads compared to conventional IAM channel estimator. The developed C-FBMC/OQAM system demonstrate better robustness against frequency selective fading channels compared to conventional FBMC/OQAM system

due to subcarrier-wise intrinsic interference cancellation by adopting the concept of the repeated frame.

REFERENCES

[1] M. Bellanger, "FBMC physical layer: A primer," *PHYDYAS FP7 Project Document,* Jan. 2010.

[2] B. Farhang-Boroujeny, "OFDM versus filter bank multicarrier," *IEEE Signal Process. Mag,* vol. 28, no. 3, pp. 92-112, May. 2011.

[3] A. I. Pérez-Neira et al., "MIMO signal processing in offset-QAM based filter bank multicarrier systems," *IEEE Trans. Signal Process,* vol. 64, no. 21, pp. 5733-5762, Nov. 2016.

[4] P. Siohan, C. Siclet and N. Lacaille, "Analysis and design of OQAM-OFDM systems based on filterbank theory," *IEEE Trans. Signal Process,* vol. 50, no. 5, pp. 1170-1183, May. 2002.

[5] A. Zafar, L. Zhang, P. Xiao, and M. A. Imran, "Spectrum efficient MIMO-FBMC System using Filter Output Truncation," *IEEE Trans. Veh. Technol,* vol. 67, no. 3, pp. 2367-2381, Mar. 2018.

[6] A. Aminjavaheri, A. Farhang, and B. Farhang-Boroujeny, "Filter bank multicarrier in massive MIMO: analysis and channel equalization," in *IEEE Trans. Signal Process,* vol. 66, no. 15, pp. 3987-4000, Aug. 2018.

[7] D. Qu, S. Lu, and T. Jiang, "Multi-block joint optimization for the peak to- average power ratio reduction of FBMC-OQAM signals," *IEEE Trans. Signal Process,* vol. 61, no. 7, pp. 1605-1613, Apr. 2013.

[8] L. Wen et al., "Joint sparse graph for FBMC/OQAM systems," *IEEE Trans. Veh. Technol,* vol. 67, no. 7, pp. 6098-6112, Jul. 2018.

[9] D. L. Wasden, H. Moradi, and B. Farhang-Boroujeny, "Design and implementation of an underlay control channel for cognitive radios," *IEEE J. Sel. Areas Commun,* vol. 30, no. 10, pp. 1875-1889, Nov. 2012.

[10] J. Denis, M. Pischella, and D. Le Ruyet, "Energy-efficiency-based resource allocation framework for cognitive radio networks with FBMC/OFDM," *IEEE Trans. Veh. Technol,* vol. 66, no. 6, pp. 4997-5013, Jun. 2017.

[11] Q. Bodinier, F. Bader, and J. Palicot, "On spectral coexistence of CP-OFDM and FB-MC waveforms in 5G networks," *IEEE Access,* vol. 5, pp. 13883-13900, 2017.

[12] H. Bogucka, P. Kryszkiewicz, and A. Kliks, "Dynamic spectrum aggregation for future 5G communications," *IEEE Commun. Mag,* vol. 53, no. 5, pp. 35-43, May. 2015.

[13] O. Font-Bach et al., "When SDR meets a 5G candidate waveform : agile use of fragmented spectrum and interference protection in PMR networks," *IEEE Trans. Wireless Commun,* vol. 22, no. 6, pp. 56-66, Dec. 2015.

[14] Y. Medjahdi, M. Terre, D. L. Ruyet, D. Roviras, and A. Dziri, "Performance analysis in the downlink of asynchronous OFDM/FBMC based multi-cellular networks," *IEEE Trans. Wireless Commun,* vol. 10, no. 8, pp. 2630-2639, Aug. 2011.

[15] "Physical layer for dynamic spectrum access and cognitive radio (PHYDYAS)," [Online]. Available: http://www.ict-phydyas.org/.

[16] "5th Generation non-orthogonal waveforms for asynchronous signaling (5GNOW)," [Online]. Available: http://www.5gnow.eu/.

[17] "Mobile and wireless communications enablers for the twenty-twenty information society (METIS)," [Online]. Available: https://www.metis2020.com/.

[18] D. Kong, D. Qu, and T. Jiang, "Time domain channel estimation for OQAM-OFDM systems: algorithms and performance bounds," *IEEE Trans. Signal Process,* vol. 62, no. 2, pp. 322-330, Jan. 2014.

[19] W. Cui, D. Qu, T. Jiang, and B. Farhang-Boroujeny, "Coded auxiliary pilots for channel estimation in FBMC-OQAM systems," *IEEE Trans. Veh. Technol,* vol. 65, no. 5, pp. 2936-2946, May. 2016.

[20] D. Qu, F. Wang, Yan Wang, T. Jiang, and B. Farhang-Boroujeny. "Improving spectral efficiency of FBMC-OQAM through virtual symbols," *IEEE Trans. Wireless Commun,* vol. 16, no. 7, pp. 4204-4215, Jul. 2017.

[21] E. Kofidis C. Chatzichristos A. L. F. de Almeida "Joint channel estimation/data detection in MIMO-FBMC/OQAM systems—A tensor-based approach," *Proc. 25th Eur. Signal Process. Conf.(EUSIPCO),* pp. 420-424, 2017.

[22] R. Zakaria D. Le Ruyet Y. Medjahdi "On ISI cancellation in MIMO-ML detection using FBMC/QAM modulation" *Proc. IEEE Int. Symp. Wireless Commun. Syst. (ISWCS),* pp. 949-953, Aug. 2012.

[23] D. Qu, Y. Qiu, T. Jiang, "Finer SVD-based beamforming for FBMC/OQAM systems", *Proc. IEEE Glob. Commun. Conf.,* pp. 1-7, Dec. 2016.

[24] D. Na and K. Choi, "Intrinsic ICI-Free Alamouti coded FBMC," *IEEE Commun. Lett,* vol. 20, no. 10, pp. 1971-1974, Oct. 2016.

[25] C. Lélé, J. Javaudin, R. Legouable, A. Skrzypczak, P. Siohan, "Channel estimation methods for preamble-based OFDM/OQAM modulations", *European Trans. Telecommun.,* vol. 19, no. 7, pp. 741-750, Nov. 2008.

[26] C. Lélé, P. Siohan, R. Legouable, R. Legouable, "2 dB better than CP-OFDM with OFDM/OQAM for preamble-based channel estimation",*Proc. IEEE Int. Conf. Commun. (ICC),* pp. 1302-1306, Jun. 2008.

[27] E. Kofidis, D. Katselis, A. Rontogiannis, and S. Theodoridi, "Preamble-based channel estimation in OFDM/OQAM systems: a review," *Signal Processing,* vol. 93, no. 7, pp. 2038-2054, Jul. 2013.

[28] E. Kofidis, D. Katselis, "Improved interference approximation method for preamble-based channel estimation in FBMC/OQAM", *19th Eur. Signal Process. Conf. (EUSIPCO),* Aug. 29–Sep. 2 2011.

[29] H. Wang, W. Du, L. Xu, "Novel preamble design for channel estimation in FBMC/OQAM systems", *KSII Trans. Internet Inf. Syst.,* vol. 10, no. 8, pp. 3672-3688, Aug. 2016.

[30] H. Wang, L. Xu, X. Wang, and S. Taheri, "Preamble design with interference cancellation for channel estimation in MIMO-FBMC/OQAM systems," *IEEE Access,* vol. 6, pp. 44072-44081, 2018.

[31] E. Kofidis "Preamble-based estimation of highly frequency selective channels in FBMC/OQAM systems" , *IEEE Trans. Signal Process.* vol. 65 no. 7 pp. 1855-1868 Apr. 2017.

[32] M. A. AboulDahab, M. M. Fouad, R. A. Roshdy, "A proposed preamble based channel estimation method for FBMC in 5G wireless channels," *Proc. 35th Nat. Radio Sci. Conf. (NRSC),* pp. 140-148, Mar. 2018.

[33] J.-P. Javaudin, D. Lacroix, A. Rouxel, "Pilot-aided channel estimation for OFDM/OQAM", *Proc. IEEE Vehic. Technol. Conf. (VTC),* vol. 3, pp. 1581-1585, Apr. 2003.

[34] C. Kim, Y. H. Yun, K. Kim, and J. Seol, "Introduction to QAM-FBMC: from waveform optimization to a system design," *IEEE Commun. Mag,* vol. 54, no. 11, pp. 66-73, Nov. 2016.

[35] H. Nam, M. Choi, S. Han, C. Kim, S. Choi, and D. Hong, "A new filter-bank multicarrier system with two prototype filters for QAM symbols transmission and reception," *IEEE Trans. Wireless Commun,* vol. 15, no. 9, pp. 5998-6009, Sept. 2016.

[36] H. Han, H. Kim, N. Kim, and H. Park, "An enhanced QAM-FBMC scheme with interference mitigation," *IEEE Commun. Lett,* vol. 20, no. 11, pp. 2237-2240, Nov. 2016.

[37] J. Kim, Y. Park, S. Weon, J. Jeong, S. Choi, and D. Hong, "A new filter-bank multicarrier system: the linearly processed FBMC system," *IEEE Trans. Wireless Commun,* vol. 17, no. 7, pp. 4888-4898, Jul. 2018.

[38] J. Du P. Xiao J. Wu Q. Chen "Design of isotropic orthogonal transform algorithm-based multicarrier systems with blind channel estimation," *IET Commun.* vol. 6 no. 16 pp. 2695-2704 Nov. 2012.

[39] M. Caus and A. I. Pérez-Neira, "Multi-stream transmission for highly frequency selective channels in MIMO-FBMC/OQAM systems," *IEEE Trans. Signal Process,* vol. 62, no. 4, pp. 786-796, Feb. 2014.

[40] E. Kofidis, "Preamble-based estimation of highly frequency selective channels in FBMC/OQAM systems," *IEEE Trans. Signal Process,* vol. 65, no. 7, pp. 1855-1868, Apr. 2017.

[41] J. Arunprakash and G. Reddy, "Discrete ambiguity function based analysis of filter bank multicarrier systems" *IETE Technical Review,* vol. 32, no.5, pp. 330-346, 2015.

[42] M. Renfors, T. Ihalainen, T. H. Stitz, "A block-Alamouti scheme for filter bank based multicarrier transmission", *Proc. 2010 European Wireless Conf.,* pp. 1038-1041.

[43] T. Innovations, "LTE in a nutshell", 2010.

[44] R. Jain, Channel Models A Tutorial., WiMAX Forum AATG, Feb. 2007.